2018

# EVALUATION OF THE ACCURACY OF MACHINE REPORTED CAN DATA FOR ENGINE TORQUE AND SPEED (J1939)

Rodney A. Rohrer
*University of Nebraska - Lincoln*, rrohrer2@unl.edu

Joe D. Luck
*University of Nebraska-Lincoln*, jluck2@unl.edu

Santosh K. Pitla
*University of Nebraska-Lincoln*, spitla2@unl.edu

Roger M. Hoy
*University of Nebraska - Lincoln*, rhoy2@unl.edu

# EVALUATION OF THE ACCURACY OF MACHINE REPORTED CAN DATA FOR ENGINE TORQUE AND SPEED

R. A. Rohrer, J. D. Luck, S. K. Pitla, R. Hoy

**ABSTRACT.** *Most modern off-road machinery use embedded electronic controllers connected to a controller area network (CAN) to broadcast machine information for on-board processes and diagnostics. Commercially available tools can record CAN data for a variety of research and commercial uses. For agricultural tractors, there is an opportunity to create advanced test procedures that are more representative of field operations and that could supplement existing machine performance tests, such as the OECD Code 2 Standard Code for the Official Testing of Agricultural and Forestry Tractor Performance. CAN parameters provide an efficient way to collect tractor performance data during field operations. However, the accuracy of CAN messages is not known, and little information was found in the literature regarding the accuracy of CAN messages or validation of reported signals. The objective of this study was to investigate the accuracy of net engine torque as calculated from several relevant CAN channels by comparing it to torque measured with a calibrated laboratory dynamometer. Results of this study indicate statistically significant differences between calculated and measured net engine torque, although there was a strong correlation. Recommendations for future work include replicating this study on more and different engines that report actual engine percent torque - fractional (SPN 4154) and estimated engine parasitic losses - percent torque (SPN 2978). This would provide higher-resolution torque estimates that may help explain the torque differences observed in this study.*

***Keywords.*** *Accuracy, Agricultural machinery, Calibration, Controller area network, CAN bus, Data acquisition, Diesel engine, Dynamometer, Equipment performance, J1939, Machinery, Off-road vehicles, Power take-off, PTO, Tractors, Torque.*

Most modern off-road machinery is configured with networked electronic controllers that broadcast machine information used for on-board processes and diagnostics. The physical controller area network (CAN) and data structure typically conform to industry standards, such as SAE J1939 and ISO 11783, to ensure compatibility between hardware devices. Tools are commercially available that can capture CAN data and log it to a file, or transfer it to a cloud server, for a variety of research and commercial uses. For researchers studying machine performance and efficiency, CAN data provide a convenient means of data collection in which the complexities of auxiliary sensors and data acquisition systems can be avoided (Al-Aani et al., 2016; Pitla et al., 2014). Equipment owners and operators can optimize machinery management and logistics with information gleaned from CAN data from their own operations (Darr, 2012; Pitla et al., 2014). Machinery manufacturers use data collected from controller area networks to better understand equipment use profiles, loads, and duty cycles (Estino, 2017). Machine use characteristics extracted from these data are used for machine development to ensure that future designs meet customer needs. The electronic and distributed system architecture also lends itself to machine automation in which intelligent machines can use J1939 messages in lieu of physical sensors (Darr et al., 2005; Polcar et al., 2016).

CAN data are being used to support advanced test procedures for evaluating engine emissions and machine performance. Portable emissions measurement systems (PEMS) that use J1939 parameters are being developed to measure engine emissions during use, referred to as "in-service conformity," instead of relying on laboratory tests based on simulated operation cycles (Bonnel et al., 2013). The U.S. Environmental Protection Agency (USEPA, 2012) and the California Air Resources Board have established regulations (California, 2016) that also reference SAE J1939 parameters for use in emissions testing. According to SAE International, "beginning in 2016, HD-OBD (heavy-duty onboard diagnostics) requires reporting of engine torque to portable emissions measurement system (PEMS) equipment that is representative of torque as measured by the engine dynamometer during the emissions certification process" (SAE, 2016a).

For agricultural tractors, there is an opportunity to create advanced test procedures that are more representative of field operations to better assess machine efficiency. This

Submitted for review in December 2017 as manuscript number MS 12754; approved for publication by the Machinery Systems Community of ASABE in August 2018.

The authors are **Rodney A. Rohrer,** Research Engineer, **Joe D. Luck,** Associate Professor, **Santosh K. Pitla,** Assistant Professor, and **Roger Hoy,** Professor, Department of Biological Systems Engineering, University of Nebraska, Lincoln, Nebraska. **Corresponding author:** Rodney Rohrer, 134 Splinter Labs, University of Nebraska, Lincoln, NE 68583; phone: 402-472-2442; email: rrohrer2@unl.edu.



Vol. 61(5): 1547-1557  ISSN 2151-0032 https://doi.org/10.13031/trans.12754 

could supplement existing machine performance tests, such as the OECD Code 2 Standard Code for the Official Testing of Agricultural and Forestry Tractor Performance. Data from actual field operations would be needed to determine the magnitude, duration, and combination of loads to apply with test equipment. The most direct way to measure in-field loads is by installing analog sensors on tractors and implements, e.g., a load cell and radar to measure drawbar pull and ground speed, torque and speed sensors to measure PTO power, and flowmeters and pressure sensors to measure hydraulic power. However, disadvantages associated with using analog sensors for in-field measurements include:

- Analog sensors and data acquisition systems are expensive and time-consuming to install, especially if they need to be replicated on many tractors and implements.
- Analog sensors need to withstand shock, vibration, dust, moisture, and sometimes harsh temperatures in the off-road equipment operating environment.
- Analog sensors can be a hindrance for the tractor operator.
- Equipment configurations may need to be altered to accommodate sensors.
- Travel to the equipment is required for sensor installation and maintenance of the data acquisition system.
- Analog data may have to be merged with data from other sources, including tractor and implement CAN and global navigation satellite systems (GNSS).

Although there are advantages to using CAN data instead of analog measurements, a primary concern is the accuracy of the CAN parameters. Many CAN parameters are based on on-machine sensors for which traceable calibration is not available, or the parameters of interest may be based on software tables or calculations and are not actually measured directly. Before pursuing large-scale field data collection based on CAN data, some effort is required to verify the accuracy of the parameters of interest. A study by Marx (2015) investigating the accuracy of CAN-reported fuel consumption showed the fuel consumption to be within ±5% of that measured with a laboratory flowmeter for all steady-state loads and within ±1% for high-load operations at steady state. Little additional information was found in the literature regarding the accuracy of CAN messages or validation of reported signals.

When studying machine performance, a key parameter of interest is net engine torque. Net engine torque can be measured with a laboratory dynamometer, but it is impractical to directly measure net torque for engines installed in machines or to remove the engines from the machines for laboratory testing. Agricultural tractors configured with a power take-off (PTO) can be connected to a dynamometer to measure power output at the PTO; however, due to parasitic losses, this is not a direct indication of net engine power. Rencin and Polcar (2016) used dynamometer testing to correlate PTO power with CAN-reported engine percent torque with the intent of using CAN parameters to determine tractor engine power during in-field use. While those researchers recognized the need to verify the accuracy of CAN-reported information, and they were able to create a matrix from which to interpolate PTO power based on engine speed and engine percent torque, they did not use related CAN messages from which net engine torque can be calculated, as defined in SAE J1939. The relationship between PTO power and engine percent torque would be valid only for cases that do not include drawbar or hydraulic loads. To determine the power transferred through each load path, independent measurements would be required for each power outlet, or a combination of measured power and net engine torque would be needed to determine power output from all modes.

Many CAN parameters are required to fully understand machine use, performance, and efficiency, all of which should be evaluated for accuracy before investing in large-scale data collection or using the data to draw significant conclusions. The objective of this research was to evaluate the accuracy of net engine torque as determined from J1939 CAN messages.

## MATERIALS AND METHODS

### ENGINE TORQUE MEASUREMENT

An experiment was performed to determine how closely net engine torque based on J1939 CAN parameters correlated with torque measured with a dynamometer. The hardware used for this experiment included a Tier 3, four-cylinder, industrial diesel engine (4045HG485, John Deere, Waterloo, Iowa) fitted with a manually actuated clutch (SP111HP3, TwinDisc, Inc., Racine, Wisc.) that was connected to an eddy current dynamometer (Dynamatic 1519DG, Dyne Systems, Jackson, Wisc.), as shown in figure 1. The diesel engine had 4.5 L displacement with nominal power of 115 kW at 2400 rpm. The dynamometer was equipped with a dual-output load cell (1110-JW, Interface, Inc., Scottsdale, Ariz.), speed sensor (EP10234, Sensoronix, Irvine, Cal.), and eddy current dynamometer controller (EC1001C, DynoOne, Edinburgh, Ind.). The dual-output load cell contained two sets of sensors to provide load signals to the dynamometer controller and to the data acquisition system. A schematic of the engine and dynamometer used in this study is shown in figure 2.

Dynamometer torque was calibrated in increments of 203 N·m (150 lbf·ft) with weights certified by the Nebraska Department of Agriculture Weights and Measures. As calibration weights were incrementally applied, the load cell voltage was recorded as an average over a 20 s duration at constant load. This process was repeated as the weights were incrementally removed. The load cell voltages for corresponding loading and unloading points were averaged together to account for hysteresis from the loading direction. A calibration table was made from the applied loads and corresponding load cell voltages. The calibration table was applied to the load cell signal in the data acquisition software, and weights were applied again to verify the calibration. The results are shown in table 1 along with the percent error for each load point. The largest error was 0.19%, and the average error was 0.11%. The values from table 1 are shown graphically in figure 3, where a trend line was fit to the average scaled values. The coefficient of determination ($R^2$ value) of 1.00 was an indication of strong correlation between the applied load and measured load.

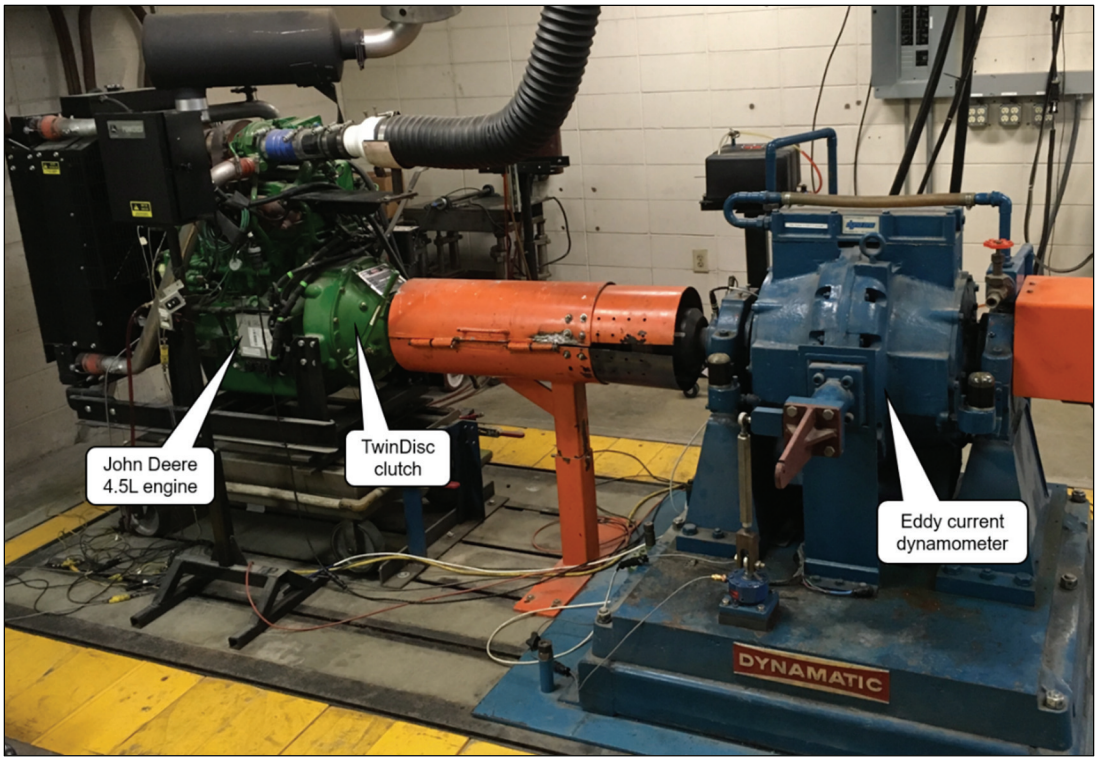


**Figure 1. Engine and dynamometer configuration.**

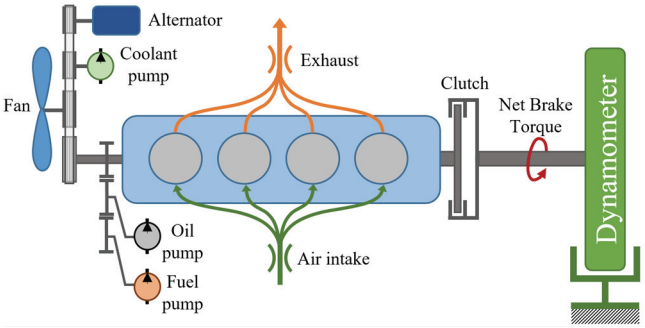


**Figure 2. Power system schematic.**

**Table 1. Summary of dynamometer torque calibration results.**

| | DAQ Measurements | | | |
|---|---|---|---|---|
| Applied Load (N·m) | Loading (N·m) | Unloading (N·m) | Average Measured Load (N·m) | Error (%) |
| 0.0 | 0.04 | 0.06 | 0.05 | |
| 203.37 | 203.21 | 203.77 | 203.49 | 0.06 |
| 406.75 | 406.04 | 406.27 | 406.16 | -0.15 |
| 610.12 | 608.54 | 609.32 | 608.93 | -0.19 |
| 813.49 | 812.09 | 812.07 | 812.08 | -0.17 |

The data acquisition system, shown in figure 4, consisted of a National Instruments (NI) cDAQ-9174 USB chassis equipped with the following modules:

- NI 9862 one-port high-speed/FD NI-XNET CAN C Series module.
- NI 9219 universal analog input, 24-bit, 100S/s/ch, 4-channel module.
- NI 9401 5V/TTL, bidirectional digital I/O, 8-channel module.

A custom LabVIEW program was created to view and record data during the experiment. The data acquisition system had three inputs: J1939 CAN, dynamometer torque (analog signal), and dynamometer speed (digital signal). The LabVIEW software was configured to use the same sample clock for all signals to ensure synchronization of the collected data. Data were collected in waveform format at a rate of 20 Hz and streamed to a LabVIEW technical data management streaming (.tdms) log file with no additional signal conditioning.

It should be noted that J1939 parameter groups are broadcast at varying rates, and some are updated based on engine crank angle, or when a state change occurs, rather than at a specific time interval (SAE, 2016b). To ensure time synchronization of CAN signals with analog signals, the same analog sample clock was used to start the CAN data task and to resample CAN data at the same rate as the analog signals. A CAN database (.dbc) file was used with NI-XNET to decode the J1939 messages in real-time before writing the parameters to the log file.

## J1939 CAN Messages for Torque Estimation

As described in SAE J1939-71 (SAE, 2016b) and SAE J1939DA (digital annex) (SAE, 2016a), static messages available in parameter group number (PGN) 65251 EC1 (engine configuration 1) provide information about the general shape of the engine torque curve and engine reference torque. Engine configuration data and associated suspect parameter numbers (SPN) retrieved from the CAN bus for the John Deere 4.5 L engine used in this study are shown in table 2. Torque messages on the CAN bus were reported as a percentage of engine reference torque, which is the 100% reference value for all defined engine torque parameters (SAE, 2016a). For the engine used in this study, the engine

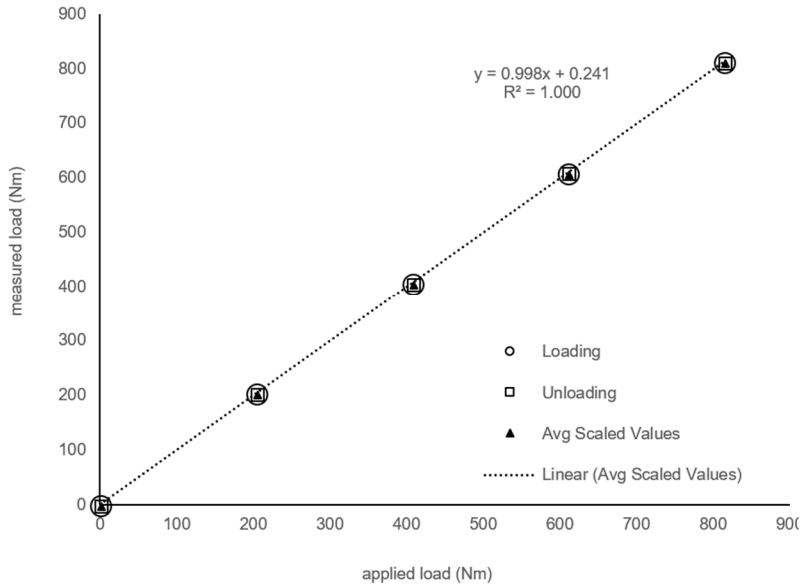


**Figure 3. Cross-plot of measured versus applied dynamometer torque loads after calibration.**

**Figure 4. National Instruments cDAQ-9174 with modules.**

**Table 2. PGN 65251 EC1 messages from John Deere 4.5 L engine.**

| Parameter | SPN | Units | Reported Value |
|---|---|---|---|
| EngSpeedAtIdlePoint1 | 188 | rpm | 800 |
| EngSpeedAtPoint2 | 528 | rpm | 2470 |
| EngSpeedAtPoint3 | 529 | rpm | 500 |
| EngSpeedAtPoint4 | 530 | rpm | 1156.625 |
| EngSpeedAtPoint5 | 531 | rpm | 1813.25 |
| EngSpeedAtHighIdlePoint6 | 532 | rpm | 2470 |
| EngPercentTorqueAtIdlePoint1 | 539 | % | 77 |
| EngPercentTorqueAtPoint2 | 540 | % | 77 |
| EngPercentTorqueAtPoint3 | 541 | % | 77 |
| EngPercentTorqueAtPoint4 | 542 | % | 90 |
| EngPercentTorqueAtPoint5 | 543 | % | 89 |
| EngReferenceTorque | 544 | N·m | 700 |

reference torque was 700 N·m.

Torque values reported as percentages of engine reference torque were converted to engineering units using equation 1:

**Table 3. Stationary engine torque map as described in PGN 65251 EC1 for the John Deere 4.5 L engine used in this study.**

| Point | Speed (rpm) | Torque (%) | Torque (N·m) |
|---|---|---|---|
| Point 1 | 800 | 77 | 539 |
| Point 2 | 2470 | 77 | 539 |
| Point 3 | 500 | 77 | 539 |
| Point 4 | 1156.625 | 90 | 630 |
| Point 5 | 1813.25 | 89 | 623 |
| High Idle Point 6 | 2470 | 0 | 0 |

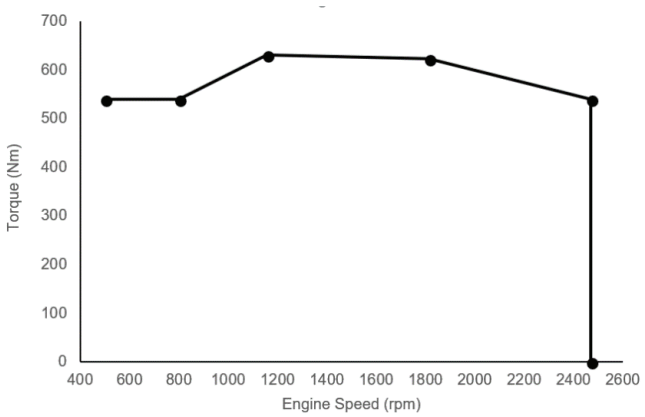


**Figure 5. Graph of stationary engine torque map as described in PGN 65251 EC1 for the John Deere 4.5 L engine.**

$$\text{Torque (N}\cdot\text{m)} = \frac{\text{Percent torque (\%)}}{100} \times \text{Engine reference torque (N}\cdot\text{m)} \quad (1)$$

The stationary engine torque map as described in PGN 65251 EC1 for the John Deere 4.5 L engine used in this study is shown in table 3 and figure 5.

Static engine friction torque values that correspond to the stationary engine torque values given in PGN 65251 EC1 are defined in PGN 64743 EC3 (engine configuration 3), but EC3 friction torque values were not reported for this engine.

SAE J1939DA defines a set of messages in PGN 64912 (advertised engine torque curve) that may have been helpful in understanding the torque characteristics of this engine, but these messages were also not reported for this engine.

SAE J1939 defines net engine brake torque (power) as: "The measured torque (or power output) of a 'fully equipped' engine. A fully equipped engine is an engine equipped with accessories necessary to perform its intended service. This includes, but is not restricted to, the basic engine, including fuel, oil, and cooling pumps, plus intake air system, exhaust system, cooling system, alternator, and starter, emissions, and noise control. Accessories which are not necessary for the operation of the engine, but may be engine mounted, are not considered part of a fully equipped engine. These items include, but are not restricted to, power steering pump systems, vacuum pumps, and compressor systems for air conditioning, brakes, and suspensions" (SAE, 2016b).

Net engine brake torque is equal to gross engine torque minus the torque required to overcome engine friction and to drive engine accessories. These accessory loads, which are necessary for operation of the engine but do not contribute to useful work, are often described as parasitic loads. Engine parasitic loads can include:

- Engine friction
- Air intake restrictions
- Exhaust system restrictions
- Fuel pump
- Oil pump
- Coolant pump
- Alternator
- Fan
- Other accessories such as air compressor, air conditioning compressor, etc.

SAE J1939 defines several messages that can be used to calculate net engine brake torque. These messages and their abbreviated definitions from SAE J1939DA are given below:

**Actual Engine - Percent Torque (SPN 513):** The calculated output torque of the engine. The data are transmitted in indicated torque as a percentage of the reference engine torque. The engine percent torque value will not be not less than zero, and it includes the torque developed in the cylinders required to overcome friction.

**Actual Engine - Percent Torque (Fractional) (SPN 4154):** This parameter is used in combination with SPN 513. The resulting actual engine torque is calculated by adding these two parameters.

**Nominal Friction - Percent Torque (SPN 514):** The calculated torque that indicates the amount of torque required by the basic engine itself and the torque losses of accessories. SPN 514 includes the frictional and thermodynamic losses of the engine, pumping torque loss, and the torque losses of the fuel, oil, and cooling pumps. The realization can be done with a map dependent on engine speed and engine temperature and an offset value for additional torque losses. SPN 2978 describes the possible inclusion of engine parasitic losses, such as cooling fan, etc., in this parameter. For applications that are subject to HD-OBD regulations in 2016 or later, estimated parasitic losses are no longer included in SPN 514 and must be included in SPN 2978.

**Estimated Engine Parasitic Losses - Percent Torque (SPN 2978):** The calculated torque that indicates the estimated amount of torque loss due to engine parasitic loads, such as cooling fan, air compressor, air conditioning, etc. It is expressed as a percentage of the engine reference torque.

The engine used in this study reported SPN 4154 as a constant value of 1.875%, which was outside the defined range of 0% to 0.875% for this parameter. This parameter has a resolution of 0.125% per bit and an offset of zero. When the reported value of 1.875% was divided by 0.125% per bit, the result was $15_{10}$ or $1111_2$. Per SAE J1939DA, values of $1000_2$ to $1111_2$ indicate that this message is not available, so it was not considered in subsequent torque calculations in this study.

SPN 2978 was reported as a constant value of 130%, which was outside the defined range of -125% to 125% for this parameter. The parameter has a resolution of 1% per bit and an offset of -125%. When the -125% offset was applied to the 130% reported value, the result was $255_{10}$ or $FF_{16}$. SAE J1939 specifies that undefined bytes should be sent as $FF_{16}$, indicating that this message was not defined for this engine; therefore, it was not used in subsequent torque calculations (SAE, 2016a; Walter and Walter, 2016)

When the reported value for SPN 2978 is equal to $FB_{16}$, it indicates that all parasitic losses calculated for the engine are included in the nominal friction percent torque (SPN 514) (SAE, 2016a). As described in the previous paragraph, the reported value for SPN 2978 was not defined for this engine and does not show that the parasitic load for the fan was included in the data for SPN 514.

As described above, gross torque was characterized by the actual engine percent torque (SPN 513). Parasitic loads, with exception of the cooling fan, are included in the nominal friction percent torque (SPN 514). Engine net brake torque was calculated from CAN parameters by subtracting the nominal friction torque from the actual engine torque and multiplying by the engine reference torque, as shown in equation 2:

$$\begin{aligned}\text{Net torque } (\mathrm{N \cdot m}) = \\ &\left(\text{Actual engine percent torque}\right. \\ &\left. - \text{ Nominal friction percent torque}\right) \\ &\div 100 \times \text{Engine reference torque}\end{aligned} \tag{2}$$

## FAN TORQUE ESTIMATION

Information presented on the CAN bus indicated that fan load was not accounted for in the parameters for nominal friction percent torque or estimated engine parasitic losses, so fan load was accounted for separately. The engine sales distributor (Industrial Irrigation, Hastings, Neb.) provided fan power at various speeds, as shown in table 4. These fan load data do not correspond with the engine speeds of interest in this study, so these data were used to create a model of fan torque as a function of fan speed.

**Table 4. Fan power at various speeds provided by engine distributor. Torque was calculated from the power and speed values.**

| Speed (rpm) | Power (kW) | Torque (N·m) |
|---|---|---|
| 1476 | 1.5 | 9.7 |
| 1640 | 2.1 | 12.2 |
| 1674 | 2.3 | 13.1 |
| 1804 | 2.8 | 14.8 |
| 1836 | 3.0 | 15.6 |
| 1860 | 3.1 | 15.9 |
| 1968 | 3.7 | 18.0 |
| 2016 | 3.9 | 18.5 |
| 2040 | 4.1 | 19.2 |
| 2046 | 4.1 | 19.1 |
| 2232 | 5.3 | 22.7 |
| 2240 | 5.4 | 23.0 |
| 2244 | 5.4 | 23.0 |
| 2448 | 7.0 | 27.3 |
| 2464 | 7.2 | 27.9 |

The power consumed by the fan is proportional to the cube of fan speed (Goering et al., 2003). Because fan power is the product of torque and speed, fan torque is proportional to fan speed squared. Regression analysis using the available fan data provided a best-fit equation to use for estimating fan loads for the engine speeds of interest. A quadratic function was used to model fan torque as a function of speed. This model provided logical values for the physical system where zero torque occurs at zero speed and, as speed increases, fan torque increases at an increasing rate. Equation 3 shows the resulting model:

$$\text{Fan torque} = 4.58\text{E-}06 \times \text{Fan speed}^2 \quad (3)$$

where fan torque is in N·m and fan speed is in rpm. The coefficient of determination ($R^2$ value) of 0.999 indicated that this model for fan torque was a good fit for the original data. Additional regression statistics are shown in table 5. Figure 6 shows fan torque calculated from information provided by the engine sales distributor along with values estimated with equation 3.

The fan on this engine was belt-driven at a fixed ratio of crankshaft speed. The drive ratio between the engine crankshaft and the fan was calculated from the measured fan and engine speeds, as shown in equation 4:

**Table 5. Fan torque regression statistics for Excel LINEST regression.**

| Statistic | Symbol | Value |
|---|---|---|
| Constant base coefficient | m | 4.58E-06 |
| Coefficient of determination | $r^2$ | 0.999 |
| Standard error values for coefficients $m_n$ | $se_n$ | 9.60E-09 |
| F statistic, or F-observed value | F | 227000 |
| Regression sum of squares | $ss_{reg}$ | 5630 |
| Standard error for the *y* estimate | $se_y$ | 0.157 |
| Degrees of freedom | df | 14 |
| Residual sum of squares | $ss_{resid}$ | 0.346 |

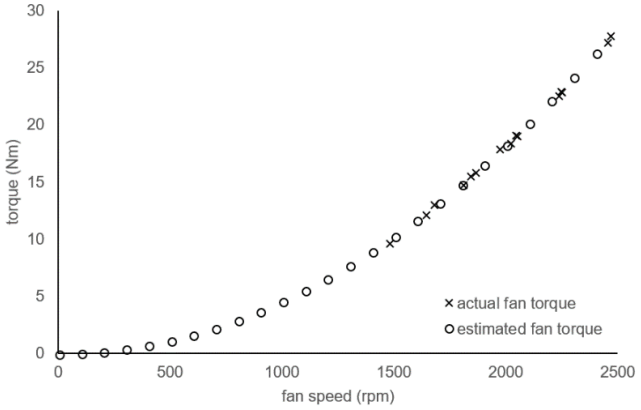


**Figure 6. Plot of actual fan torque and fan torque estimated with regression model.**

$$\frac{960 \text{ rpm Fan speed}}{800 \text{ rpm Engine speed}} = 1.20 \quad (4)$$

Fan torque was multiplied by this ratio to reflect the fan load back to the engine.

## Data Collection and Analysis

For this study, it was important to synchronize J1939 CAN data with analog data to enable valid comparisons between the reported and measured parameters. An indication of the level of synchronization was shown by comparing the J1939 reported engine speed and the measured dynamometer speed. If the signals were not well synchronized, large differences would be expected during transitions in engine speed. Figure 7

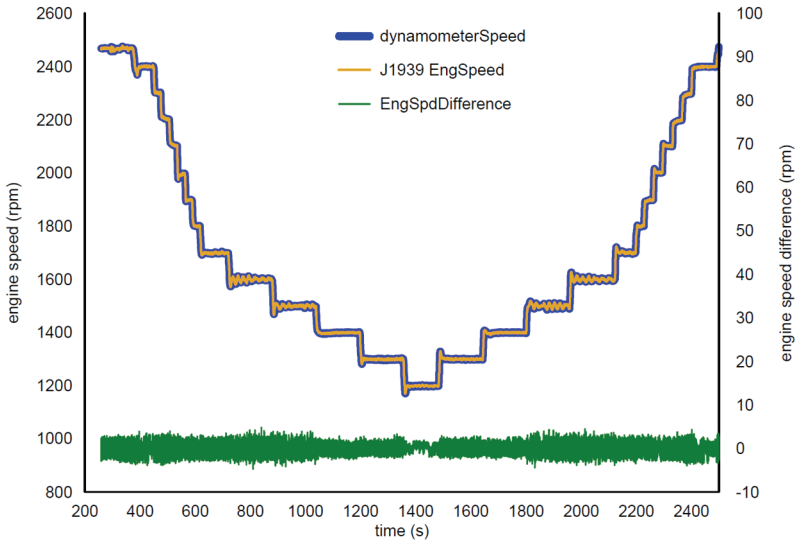


**Figure 7. Synchronization of J1939 EngSpeed (SPN 190) and analog dynamometer speed.**

shows a plot of J1939 EngSpeed (SPN 190) and dynamometer speed along with the absolute difference in these signals. The plot shows a consistent difference of approximately ±5 rpm across all speeds and a mean difference of 0.05 rpm with no distinct change in magnitude during speed transitions. Statistics related to the difference between speed signals are shown in table 6.

A cross-plot and linear regression of dynamometer speed and J1939 EngSpeed is shown in figure 8. A slope of 1 with an intercept of 0, along with an $R^2$ value of 1, are strong evidence of the correlation of these speed signals.

Early in this project, a significant amount of noise was seen in the analog torque signal, especially at speeds above 1700 rpm. Inspection of the mechanical components revealed some imbalance in the driveshaft between the clutch and dynamometer. A bearing and yoke assembly was replaced, and the driveshaft was dynamically balanced. Repair and balancing of the driveshaft helped reduce the vibration but did not eliminate the noise in the torque signal. The noise was not believed to be electrical in nature because no changes in signal quality were seen after trying different shielded instrument cables, load cells, amplifiers, and data acquisition modules. For the duration of this study, no mechanical or electrical solution was found to reduce the noise in the torque signal. We believe that the noise was caused by dynamic (mechanical) interaction between the engine, clutch, and dynamometer and interaction between the engine and dynamometer control systems.

**Table 6. Descriptive statistics for engine speed difference.**

| Statistic | Speed (rpm) |
|---|---|
| Minimum | -5.6 |
| Maximum | 4.9 |
| Mean | 0.05 |
| Standard deviation | 1.2 |

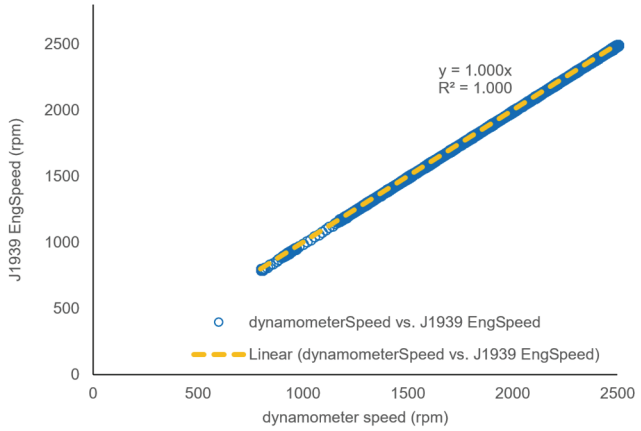


**Figure 8. Cross-plot and linear regression of dynamometer speed and J1939 EngSpeed.**

Figure 9 shows data from an engine speed sweep where speed was reduced from 2470 rpm (high idle engine speed) to 1200 rpm and back up again by adjusting the dynamometer torque. Noise in the torque signal was very apparent at engine speeds greater than 1700 rpm. Engine torque was stable from 1700 rpm down to 1300 rpm but became unstable at 1200 rpm. We believe that the torque instability at 1200 and 2400 rpm was caused by interaction between the engine and dynamometer control systems. Due to these findings, only data from 1300 to 1700 rpm were used in this study. This was less than ideal because the data of interest for field data collection includes a broader range of engine speeds. Despite the noise and regions of instability, the magnitude of the torque signal shown in figure 9 is consistent with the general shape of the torque curve shown in figure 5, where torque is nearly flat between 1200 and 1800 rpm and then slowly trends downward until reaching the steep governor curve at 2470 rpm, where it quickly goes to zero.

With the engine at full throttle, data were collected at steady-state points while decreasing and then increasing the engine speed in 100 rpm increments by changing the torque applied with the dynamometer. The engine was allowed to settle and remain at steady state for two to three minutes at each operating point. During this process, the maximum torque capability of the engine was found at each respective engine speed. At each of the same 100 rpm engine speed increments, partial load (i.e., torque) measurements were also made. For these measurements, the throttle was reduced until the engine speed was at the desired value, and then the

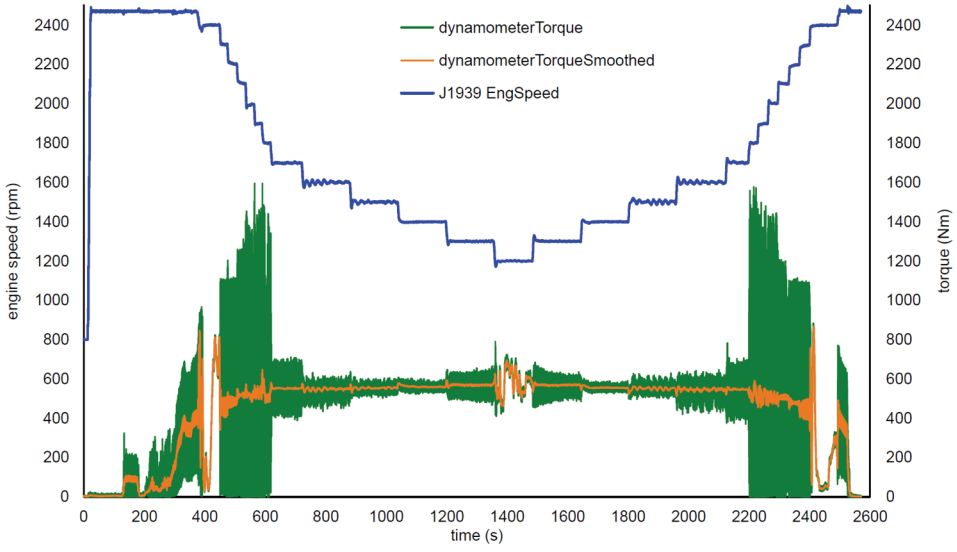


**Figure 9. Engine speed sweep at full throttle.**

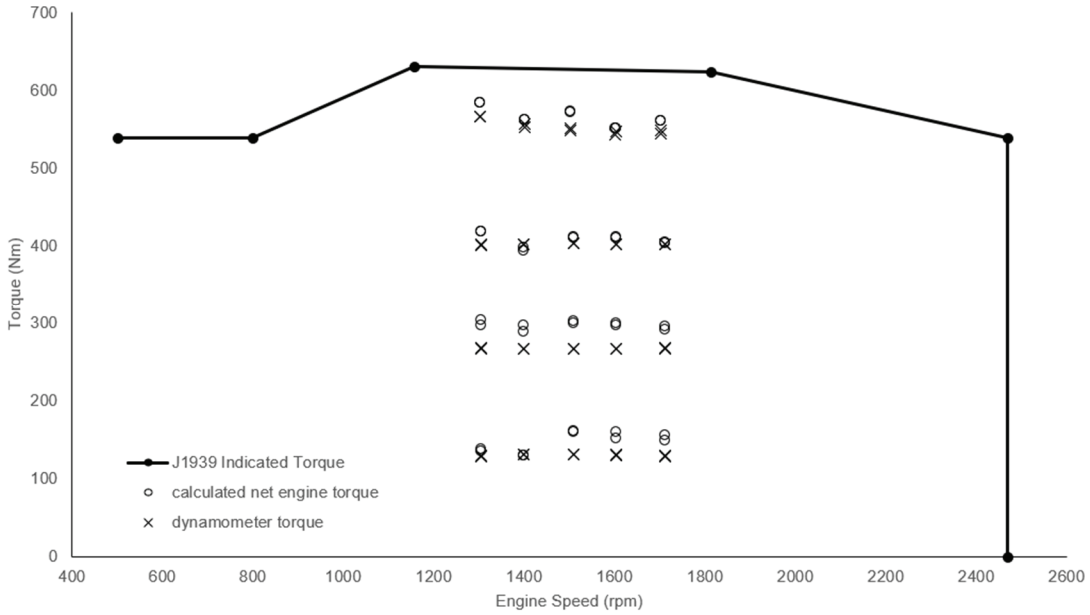


**Figure 10. Plot of torque versus engine speed showing J1939 EC1 indicated torque, calculated net engine torque, and dynamometer torque.**

dynamometer controller was used to apply varying amounts of torque. Torque was increased in 136 N·m increments, held at steady state for two to three minutes at each load increment, and then decreased at the same increments. All data were recorded with no additional filtering or signal conditioning.

The raw data were analyzed using DIAdem software. A 20-point, symmetric moving average was used to smooth the dynamometer torque signal shown in figure 9. Torque was calculated from J1939 CAN parameters as described in equation 2. An average of each signal was taken for each load point described above. Before comparison was made between the dynamometer torque and J1939 calculated net torque, the load from the cooling fan had to be accounted for. The average engine speed at each respective load point was used with equation 3 to estimate the fan torque. This estimated fan torque was reflected back to the engine using the fan drive ratio and was then subtracted from the J1939 calculated torque to get a final estimate of net engine torque. A summary of the calculated net engine torque and dynamometer torque is shown graphically in figure 10. The difference between J1939 indicated torque, reported in PGN 65251 EC1, and calculated net engine torque may be due to the lack of parameters for static engine friction defined in PGN 64743 EC3. Static engine friction parameters reported in PGN 64743 EC3 would have been subtracted from the corresponding J1939 indicated torque parameters, bringing the indicated torque curve closer to the calculated net engine torque and dynamometer torque.

Engine torque modes (SPN 899) can be monitored to better understand the torque control status of the engine (SAE, 2016a). A no-load speed sweep for the engine used in this study showed changes in engine torque mode (SPN 899) as the controlling feature changed with engine status. Three engine torque modes can be seen with this simple speed sweep, as shown in table 7 and figure 11. For data collection performed at the machine level, there may be other torque modes initiated by cruise control, torque limiting, braking system, transmission control, and other modes defined in SAE J1939 depending on engine and machine configuration. The engine used in this study was not installed in a chassis, so there were no powertrain, implement, or other external devices to interact with the engine controls.

**Table 7. Reported engine torque modes (SPN 899) for no-load speed sweep on John Deere 4.5 L engine.**

| Torque Mode | Description | Engine Speed (rpm) |
|---|---|---|
| 0 | Low-idle governor/no request (default mode) | 800 (low idle) |
| 1 | Accelerator pedal/operator selection | >800 and <2470 |
| 9 | High-speed governor | 2470 (high idle) |

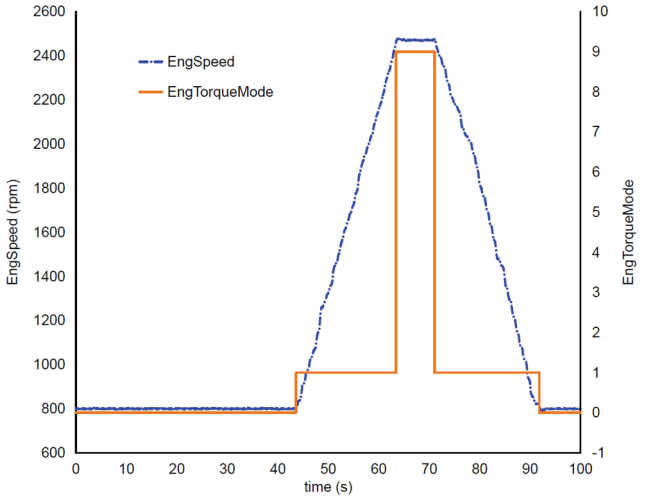


**Figure 11. Engine torque modes reported during no-load speed sweep on John Deere 4.5 L engine.**

Table 8. Descriptive statistics for torque difference (N·m).

| Statistic | All Data | Decreasing Load | Increasing Load |
|---|---|---|---|
| Minimum | -9.9 | -9.9 | -5.0 |
| Maximum | 34.8 | 31.2 | 34.8 |
| Mean | 15.3 | 14.7 | 16.0 |
| Standard deviation | 12.0 | 12.5 | 11.7 |

## RESULTS AND DISCUSSION

Descriptive statistics for the overall difference between calculated net engine torque and dynamometer torque are shown in table 8. The range of difference was 44.7 N·m for all data and, on average, calculated net engine torque was 15.3 N·m higher than dynamometer torque with a standard deviation of 12.0 N·m.

During data collection, it was noted that the torque level did not seem to return to the same value when approaching a load point from a different loading direction. A statistical t-test of the mean torque difference was completed to compare the increasing and decreasing load directions. This analysis showed that the assumption of equal variance was valid, and no statistical difference in the mean torque difference based on loading direction was found. Similarly, evaluation of the torque difference was done to compare loading direction by speed and by torque. In each case, the p-value was greater than the alpha level of 0.05. Therefore, we did not reject the null hypothesis that the mean increasing torque difference was equal to the mean decreasing torque difference and concluded that there was no difference in the data with regard to loading direction. Accordingly, all data were used in subsequent analyses, and loading direction was not considered.

Analysis of the difference between calculated net engine torque and dynamometer torque showed that the torque difference was different from zero and the calculated torque was statistically higher than the measured torque when evaluated overall and by speed and load. In each case, the p-values were less than the alpha level of 0.05; therefore, we rejected the null hypothesis that the torque difference was equal to zero and concluded that the calculated torque was statistically different from the measured torque.

All speed and load combinations were evaluated to look for trends corresponding to changes in speed and load. The p-values for some speed and load combinations were less than the 0.05 alpha level, indicating a statistically significant difference; however, for other speed and load combinations, the p-value was greater than the 0.05 alpha level, indicating no statistically significant difference between the respective loads at a given speed or between speeds at a given load. No consistent trends in torque difference were found based on speed or load. Torque difference plotted versus engine speed (fig. 12) and versus dynamometer torque (fig. 13) showed no apparent patterns or trends.

A linear regression of measured torque on calculated torque showed a strong relationship, and the $R^2$ value of 0.99 confirmed that measured torque explained 99% of the variation in calculated torque. The regression equation in figure 14 is quite close to a slope of 1 but with an offset of 23 N·m, indicating that the calculated torque was consistently higher than the measured torque.

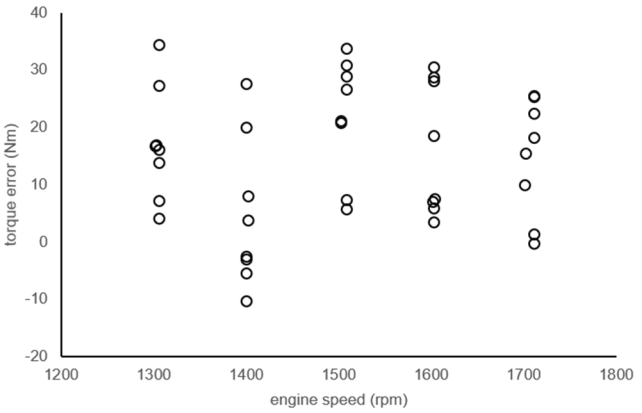


Figure 12. Torque difference versus engine speed.

### SOURCES OF ERROR

In this study, there were several potential sources of error. One source had to do with the resolution of the J1939 torque parameters that are reported as a percentage of engine reference torque. Engine reference torque for this engine was 700 N·m, which results in a resolution of 7 N·m for the two parameters used in the net engine torque calculation, i.e., actual engine percent torque and nominal friction percent torque. If the high-resolution parameter (actual engine percent torque - fractional, SPN 4154) had been available, the torque resolution would have been 0.125% of the engine reference torque, or 0.875 N·m for this engine.

Another potential source of error is that the J1939 reported torque parameters are not directly measured but instead originate from calculations or tables developed by the engine manufacturer. The conditions under which these parameters were developed are not known to users of the J1939 data and may be different from the conditions present when users are collecting data. Differences could include engine oil viscosity and intake and exhaust restrictions. In addition, the engine used for development of these parameters may have had different friction losses due to break-in and/or engine tolerances or different cooling system.

We believe that the mathematical model for the fan load was accurate based on the information available, but other characteristics of the cooling package and airflow in the local environment could affect these results. A detailed study of the cooling package and fan could be done but was not

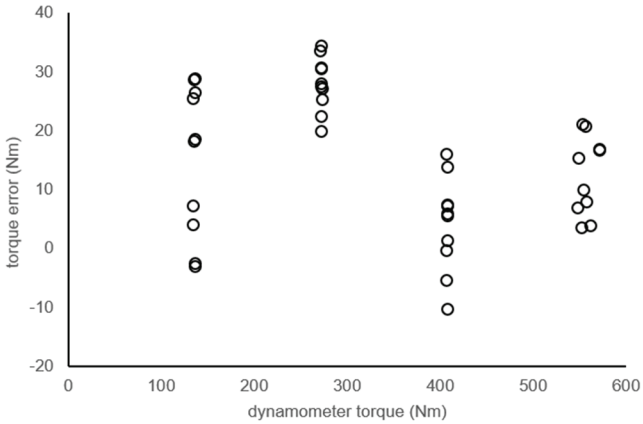


Figure 13. Torque difference versus dynamometer torque.

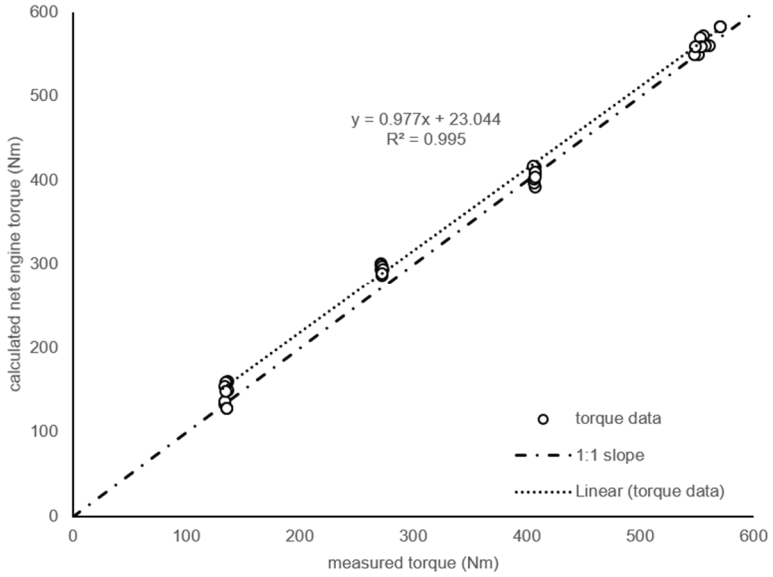


**Figure 14. Cross-plot showing correlation of calculated net torque and measured torque.**

practical for this study.

Although the dynamometer was calibrated with certified weights, some hysteresis was found in the torque signal that may have contributed to the overall torque differences in this study. The average dynamometer torque signal error was 0.11%, and the maximum error was 0.19%.

In this study, all torque measurements were attempted under steady-state load conditions to exclude any dynamic effects. Torque during load transitions was excluded from the data analysis, but mechanical vibration or other sources of signal noise may have contributed to the overall error.

## CONCLUSION

The objective of this study was to evaluate the accuracy of net engine torque determined from J1939 CAN messages. Not all parameters were reported for the engine that was used in this study, so additional work was done to model the parasitic load from the cooling fan to ensure that all loads were accounted for. On average, the J1939 calculated net engine torque was 15.3 N·m higher than the dynamometer torque, with an overall range in torque difference of 44.7 N·m. Evaluation of torque difference hysteresis based on loading direction showed no statistical difference in direction at an alpha level of 0.05 when evaluated by speed, load, and overall, indicating that loading direction can be reasonably ignored in the analysis. A linear regression of measured torque on calculated torque showed a strong relationship, as indicated by a high $R^2$ value. The difference between calculated torque and measured torque was statistically greater than zero at an alpha level of 0.05 when evaluated by speed, load, and overall. There was a significant interaction between speed and load with regard to torque difference, but no consistent trends were found.

Potential sources of error included the low resolution of the J1939 torque signals, mathematical modeling of the fan, possible error in the analog signals, signal noise, and the fact that this study used a different engine and different environmental conditions from those used to develop the J1939 torque parameters for this general engine model.

The conclusions of this study are based on results obtained from a single engine. Additional testing is recommended with different engine models from the same and different manufacturers to provide a more thorough evaluation. Testing an engine that reports actual engine percent torque - fractional (SPN 4154) and estimated engine parasitic losses - percent torque (SPN 2978) would help evaluate the significance of J1939 torque resolution and ensure that parasitic loads are accounted for by the engine manufacturer. In addition to evaluating more engines, the power of the statistical analysis could be improved by increasing the number of observations at each point of interest.

### ACKNOWLEDGEMENTS

This work was completed with the support of the Department of Biological Systems Engineering at the University of Nebraska-Lincoln and the Nebraska Tractor Test Laboratory. Additional acknowledgment to the Statistical Cross-Disciplinary Collaboration and Consulting Laboratory at the University of Nebraska-Lincoln for assistance with the data analysis.

## REFERENCES

Al-Aani, F. S., Darr, M. J., Covington, B. R., & Powell, L. J. (2016). The performance of farm tractors as reported by CAN bus messages. ASABE Paper No. 162461746. St. Joseph, MI: ASABE. https://doi.org/10.13031/aim.20162461746

Bonnel, P., Perujo, A., & Villafuerte, P. M. (2013). Non-road engines conformity testing based on PEMS. JRC Scientific and Policy Report EUR 26438 EN. Ispra, Italy: European Commission, Joint Research Centre.

California. (2016). Title 13 §1971.1: On-board diagnostic system requirements - 2010 and subsequent model-year heavy-duty engines. Sacramento, CA: California Code of Regulations.

Darr, M. J. (2012). CAN bus technology enables advanced machinery management. *Resource, 19*(5), 10-11.

Darr, M. J., Stombaugh, T. S., & Shearer, S. A. (2005). Controller area network based distributed control for autonomous vehicles. *Trans. ASAE, 48*(2), 479-490. https://doi.org/10.13031/2013.18312

Estino. (2017). Estino products and systems. Eschwege, Germany: Estino Europe. Retrieved from http://www.estino.de/products-systems/agricultural-equipment/?lang=en#toggle-id-1

Goering, C. E., Stone, M. L., Smith, D. W., & Turnquist, P. K. (2003). Cooling systems. In *Off-road vehicle engineering principles* (p. 195). St. Joseph, MI: ASABE. https://doi.org/10.13031/2013.13683

Marx, S. E. (2015). Controller area network (CAN) bus J1939 data acquisition methods and parameter accuracy assessment using Nebraska tractor test laboratory data. MS thesis. Lincoln, NE: University of Nebraska.

Pitla, S. K., Lin, N., Shearer, S. A., & Luck, J. D. (2014). Use of controller area network (CAN) data to determine field efficiencies of agricultural machinery. *Appl. Eng. Agric., 30*(6), 829-839. https://doi.org/10.13031/aea.30.10618

Polcar, A., Cupera, J., & Kumbar, V. (2016). Calibration and its use in measuring fuel consumption with the CAN bus network. *Acta Univ. Agric. Silvic. Mendelianae Brunensis, 64*, 503-507. https://doi.org/10.11118/actaun201664020503

Rencin, L., & Polcar, A. (2016). Determination of the tractor engine power in the field conditions. *Proc. 23rd Intl. PhD Students Conf.* (*MendelNet, 2016*) (pp. 916-921). Brno, Czech Republic: Mendel University, Facultry of AgriSciences.

SAE. (2016a). SAE J1939DA: Digital annex of serial control and communication heavy-duty vehicle network data. Warrendale, PA: SAE International.

SAE. (2016b). SAE J1939-71: Surface vehicle recommended practice, vehicle application layer. Warrendale, PA: SAE International.

USEPA. (2012). 40 CFR 86.010-18: On-board diagnostics for engines used in applications greater than 14,000 pounds GVWR. Washington, DC: U.S. Environmental Protection Agency.

Walter, R. P., & Walter, E. P. (2016). *Data acquisition from HD vehicles using J1939 CAN bus.* Warendale, PA: SAE International.